RSC Advances

This is an *Accepted Manuscript*, which has been through the Royal Society of Chemistry peer review process and has been accepted for publication.

Accepted Manuscripts are published online shortly after acceptance, before technical editing, formatting and proof reading. Using this free service, authors can make their results available to the community, in citable form, before we publish the edited article. This *Accepted Manuscript* will be replaced by the edited, formatted and paginated article as soon as this is available.

You can find more information about *Accepted Manuscripts* in the **Information for Authors**.

ROYAL SOCIETY OF CHEMISTRY

www.rsc.org/advances

RSC Advances

Substrate-Dependent Resistance Decrease of Graphene by Ultraviolet-Ozone Charge Doping

Lihui Liu, *[a] Zhejian Cao,[a] Wei Wang,[a] Ergang Wang,[b] Yu Cao[c] and Zhaoyao Zhan[a]

Large sheet resistance is the critical problem of graphene for application in the electronic and optoelectronic devices as transparent electrodes. Ultraviolet/Ozone (UVO) treatment is a convenient, highly effective, vacuum process and post-clean free method. This paper reveals that the effect of UVO treatment on resistance of graphene is substrate dependent, which means that the band gap and photogenerated charge carriers of the substrates under UV irritation play a key role in the doping effect. The resistance of graphene can be decreased by as much as 80% on F8BT, GaN and PTFE substrates, by 70% on PMMA substrate, by 50% on paraffin and glass substrates. Large band gap substrate (> hv) will induce p-doping effect, while small band gap substrate (< hv) with plenty of photogenerated free charge carriers will induce n-doping effect. This approach will have great impact on practical application of graphene in electronic and optoelectronic device fabrication.

1. Introduction

Graphene as the thinnest two dimensional material holds great potential in various research fields due to its remarkable electronic, optical, mechanical, and thermal properties.[1, 2] One of its most attractive applications is flexible transparent electrodes in nanoelectronic and optoelectronic devices, such as touch screens, light emitting diodes, solar cells and field-effect transistors.[3-8] Currently, indium tin oxide (ITO) is widely used as the transparent electrode material because of its low sheet resistance (10-30 Ω/sq) and high optical transmittance (>90% at 550 nm).[7] However, ITO suffers from its high cost due to the limited indium resource and stringent deposition condition, brittle and unstable property in basic or acidic environments, and poor transparency in ultraviolet (UV) and near infrared (NIR) regimes.[7, 8] Graphene possesses much better mechanical flexibility, thermal and chemical stability, and transparency over a wide wavelength range, making itself feasible to replace ITO in future devices. Nevertheless, the sheet conductivity of standard graphene remains well below commercial ITO films. The typical sheet resistance for chemical vapor deposited (CVD) single layer graphene is 0.5-5 kΩ/sq, often resulting in the reduction of device performances.

Researches have been actively pursuing to decrease the sheet resistance of graphene without significant deterioration in graphene's other properties. Doping is one of the prevailing methods to control the conductivity.[9] Graphene has been doped by structural and chemical doping. The former is realized by adding substitutional or interstitial atoms to the graphitic lattice. The doping effect is stable, but it also induces disorder in graphene, thereby reducing its carrier mobility. Chemical doping refers to the addition of atoms on the surface which involves charge transfer between the dopants and graphene.[10] Treatments by acid e.g. H_2SO_4, HNO_3, HCl,[5, 11] metal chloride e.g. $AuCl_3$, $IrCl_3$, $MoCl_3$, $OsCl_3$, $PdCl_3$, $RhCl_3$, $FeCl_3$ [12-14] and organics e.g. TFSA, $Na-NH_2$, $An-CH_3$, TPA, An-Br [15-18] are reported chemical doping methods.[19] Investigations show that the graphene sheet resistance can be decreased up to 70% and the work function simultaneously increased from 4.5 to 5.3 eV.[5, 11] However, the mobility of graphene can also be affected due to the increased scattering. Additionally, the optical transmittance can be decreased either by the band structure distortion or formation of nanoparticles on the surface, which is detrimental to optoelectronic devices.

It is highly desired to develop alternative doping approaches to increase the conductivity without reducing the mobility and optical transparency of graphene. Thus, one needs to dope the graphene while leaving the honeycomb structure unperturbed. Calculations indicate that oxygen molecules can adsorb and desorb on the graphene surface through an epoxide group formation, which involves charge transfer process and is gentle and reversible.[20, 21] Therefore, it seems that if we could find an experimental method to gently oxidize the graphene, the problem might be solved. Electron beam irradiation and oxygen plasma treatment are two well-known approaches to oxidize graphene, but they always creates sp^3 defects.[22-26] In contrast, UVO treatment is more gentle and nondestructive.[27]

[a.] Department of Microtechnology and Nanoscience, Chalmers University of Technology, Göteborg 41296, Sweden.
[b.] Department of Chemistry and Chemical Engineering, Chalmers University of Technology, Göteborg 41296, Sweden.
[c.] Department of Materials and Manufacturing Technology, Chalmers University of Technology, Göteborg 41296, Sweden.
*Corresponding author. E-mail: lihui@chalmers.se
† Electronic Supplementary Information (ESI) available: See DOI: 10.1039/x0xx00000x

RSC Advances Accepted Manuscript

Indeed, UV light assisted ozone treatment has been used to tune the work function of graphene. Unfortunately, almost all of the experimental studies show that the sheet resistance of the UVO treated graphene is several orders of magnitude higher than pristine graphene, reaching MΩ or GΩ regimes, which can be viewed as a metal-insulator transition (see the summarized references in Table S1).[28-36] Very recently, there are several reports providing some interesting results indicating that the resistance of graphene can be decreased by using UVO treatment on the traditional SiO₂ substrate.[37-39] Most of the researches focus on the effect of graphene on SiO₂ substrate or the wavelength of the utilized UV light for generation ozone molecules. However, various applications of graphene pose different requirements on the substrates, e.g. rigid or flexible, transparent or opaque, conducting or insulating, which are far beyond SiO₂ substrate. Therefore, in this work, we will pay attention to the effect of UVO treatment on the graphene doping process on various substrates, and most of them have not been under systematically investigated so far.

It has been highlighted that graphene as one of the most promising materials has been applicate in widely areas, such as electronics, photonics and energy storage. For the electronical applications, graphene is always used as the transparent conducting electronics on glass or plastic polyethylene terephthalate (PET) substrates or to fabricate transistors on the Si/SiO₂ substrate. For the photonic applications, graphene integrated with GaN or organic materials poly(9,9'-dioctylfluorene-co-benzothiadiazole) (F8BT) photodetectors are one of the most actively studied photonic devices. For the energy storage applications, graphene polytetrafluoroethylene (PTFE)-based composite is a potential supercapacitor electrode materials and graphene paraffin-based composite is a promising phase change material for power thermal storage applications. Additionally, polymethylmethacrylate (PMMA) is generally used as the mechanical supporting material in graphene transfer process. In this work, we choose these eight commonly used materials for the graphene applications as the substrates in order to systematically investigate the effect of substrate on the graphene doping via UVO treatment, and try to provide some practical investigation results. Here we transferred graphene onto these 8 different substrates via the electrochemical bubbling delamination method and investigated the effect of UVO treatment on graphene's resistance, finally find that the effect is substrate dependent. Differently from the reported always dramatically increase of the resistance, here the resistance can be decreased by as much as 80% on some substrates such as PTFE, PMMA, paraffin, F8BT, glass and GaN. It is found that the change in resistance is actually determined by the energy band structure and the photogenerated charge carriers of the substrates. Both p- and n-type doping effects can be realized in graphene via the UVO treatment. The as-developed UVO doping technique is proven to be a facile and effective method to decrease the resistance and tune the work function of graphene simultaneously, resolving one of the bottlenecks in the way towards real electronic device applications.

2. Results and discussion

2.1 Effect of the UVO treatment on the resistance of graphene on different substrates

Table 1 Target substrates used in this work and their respective bandgap values.

Substrates	Bandgap (eV)	Substrates	Bandgap (eV)
Si	1.1	PMMA	5.6
F8BT	2.1	Paraffin	8.0
GaN	3.4	Glass	9.0
PET	4.1	PTFE	9.8
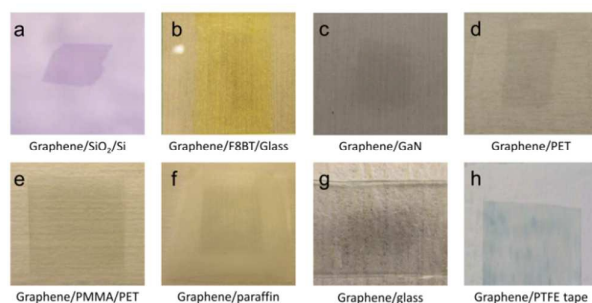
Fig. 1 Photographs of the graphene transferred on different substrates. One-time transferred graphene on (a) Si/SiO₂ substrate, (b) F8BT film, (c) GaN substrate, (d) PET substrate, (e) PMMA/PET substrate. (f) Two-time transferred graphene on a paraffin film. (g) Two-time transferred graphene transferred on glass substrate. (g) Three-time transferred graphene on PTFE film.
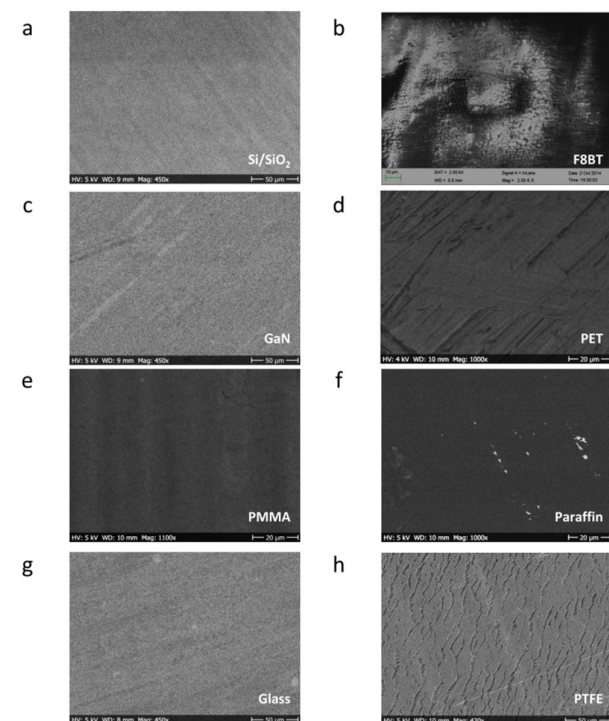
Fig. 2 TEM images for graphene on different substrates. For (a), (b), (c), (d), (e) and (g), there is one-time transferred graphene on the substrates, for (f) and (h), there are multiple transferred graphene on the substrates.

Fig. 1 shows the photographs of the graphene transferred to 8 different substrates by the electrochemical delaminated method as illustrated in the Experimental Section. The energy bandgap for each substrate is listed in Table 1. For most of the substrates which are flat and smooth, such as PET, PMMA, F8BT, SiO$_2$/Si, glass and GaN, one-time transferred graphene is enough to cover the substrate well. For paraffin and PTFE substrates, however, multilayer graphene sheets are transferred to get continuous and nonporous graphene films. The multilayer graphene transfer process is conducted as shown in Fig. S1. We can identify a region of color contrast between the graphene layer and its corresponding substrate, which gives us an initial evidence for the successful transfer. On opaque substrates, this color contrast is very pronounced,

as shown in Fig. 1a, f and h for graphene/SiO$_2$/Si, graphene/paraffin and graphene/PTFE. The color contrast is not as evident for the translucent substrates, but a larger region is still distinguishable, as shown in Fig. 1b, c, d, e and g for graphene/F8BT, graphene/GaN, graphene/PET, graphene/PMMA and graphene/glass. Furthermore, the surface morphologies and graphene continuity properties on different substrates are measured by SEM and AFM tests, and the results are listed in the Fig. 2 and S2, respectively. The thickness of the one-time transferred graphene is about 0.769 nm, indicating the CVD graphene may be double layer. And the SEM images show that all of the graphene films are continuous, indicating the electrochemical method for transferring graphene is high efficient and high quality.
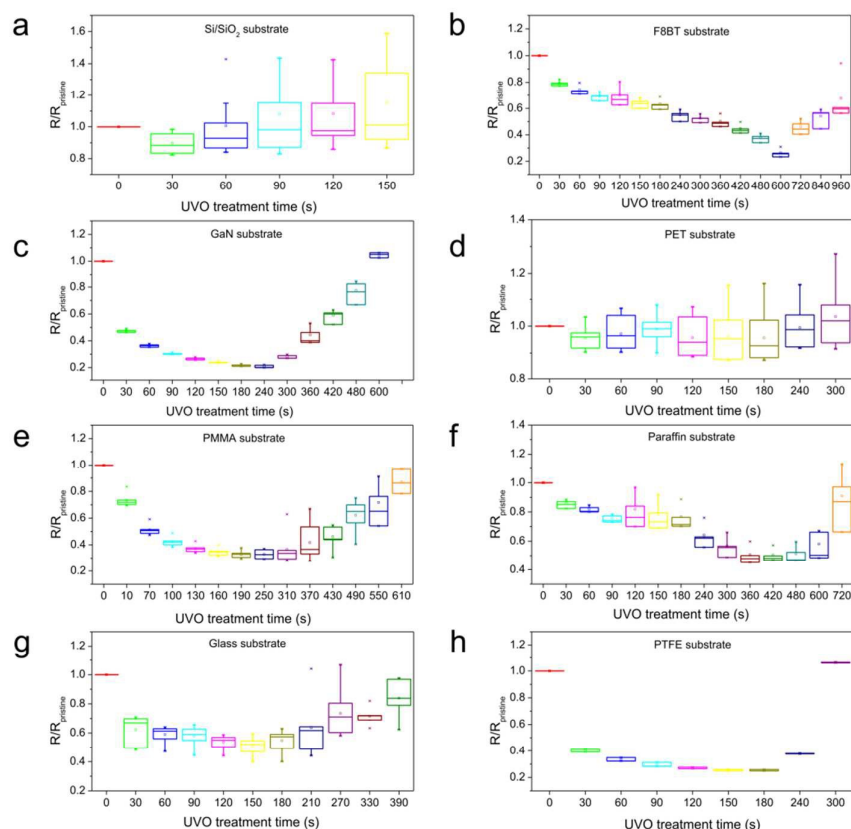
Fig. 3 Resistance change of the graphene on different substrates after the UVO treatment. All of the graphene resistance values are divided by their corresponding pristine values.

In order to measure the resistance of graphene quantitatively, we evaporate two Au electrodes with a distance of 2 mm on the graphene surface. The device configuration is presented in Fig. S3. Fig. S4 shows the evolution of resistance of graphene on different substrates versus the UVO treatment times. To obtain a good reproducibility, 2-7 devices on each substrate are fabricated and characterized. There is a variation in the resistance values among the same type of devices due to the fluctuation of process parameters in the material growth and device fabrication. However, it does not affect the overall trend of the

curves in Fig. S4. In the measurements, the contact resistance is neglected for simplicity. To see the revolution more clearly, all the resistances are normalized to the pristine value of graphene, as shown in Fig. 3. There are two stages in the evolution of graphene's resistance: short-time and long-time UVO treatment regimes. In the first stage, the resistances for all of the substrates decrease dramatically except Si/SiO$_2$ and PET. For the graphene on F8BT, GaN and PTFE substrates, the resistances decrease as much as 80% after an appropriate time of UVO treatment (600, 240 and 150 s for F8BT, GaN and PTFE, respectively). For the graphene on PMMA, the resistance

decreases by 70% after 190 s. The resistances of the graphene on paraffin (420 s) and glass (150 s) have decreased 50%. In the best case, the resistance can be brought down to 100 Ω, as shown in Fig. S4 b and c, which competes well with the best reported values by the chemical doping methods. However, in the second stage, a longer time UVO treatment can induce a sharp increase in the resistance due to the formation of a large amount of epoxide groups, which is qualitatively similar to the previously reported phenomena. Among all the substrates, the resistances of graphene on Si/SiO$_2$ and PET only increase slightly after the UVO treatment for 3 min. Note that among all the substrates we investigated in this research, only the performance of graphene on Si/SiO$_2$ has been studied comprehensively in literature. Our results on Si/SiO$_2$ are in general agreement with the previous reports, as summarized in Table S1. On the other substrates, nevertheless, there have rarely been any relevant researches reported. Further discussion on the mechanism of the charge doping induced resistance change will be presented below.

2.2 Mechanism of the substrate dependent charge doping effect on graphene by the UVO treatment

The experimental observation can be explained by the UVO induced charge doping effect involving the substrates. The ozone is produced at room temperature by UV-induced dissociation of oxygen molecules. This entails that the graphene samples are well exposed to zone molecules and oxygen radicals. In this stage, under UV illumination, hot electrons are excited in the graphene and subsequently transferred to the ozone molecules which are physisorbed on the graphene surface and have a strong electronegativity. In other words, the photogenerated electrons in graphene are extracted by the ozone molecules. This charge transfer process, however, is heavily influenced by the substrates. Additionally, we can observe the effect of ozone molecules on the surface wettability of graphene via water contact angles measurements. The water contact angles of graphene on different substrates before and after UVO treatment are presented in Figure S5. It is obvious that the graphene became

more hydrophilic after UVO treatment due to the presence of ozone molecules on the graphene surface. To quantitatively verify this charge doping effect on the three kinds of substrates, the work functions of graphene before and after the UVO treatment for different times are measured by Kelvin scanning probe microscopy (SPM). We choose three representative substrates which are flat, less sticky and, therefore, suitable for investigation: PMMA (E$_g$>hν), Si (E$_g$<hν) and GaN (E$_g$<hν). The height, surface potential and potential cross lines for the graphene on PMMA, Si/SiO$_2$ and GaN substrates before the UVO treatment are plotted in Fig. 4. The parameters of Au (the electrode material used in the electrical measurement) are simultaneously measured to generate some contrast in the images. It is found that the work function of Au is larger than that of the PFQNE-AL probe (4.1 eV) by 700 mV (4.8 eV). Similarly, the work functions of the graphene on PMMA, Si/SiO$_2$ and GaN substrates are measured to be 4.7, 4.4 and 4.6 eV, respectively. Apparently, the different work functions of graphene can be attributed to the doping effect from the substrates.[17] The value of 4.4 eV (graphene on Si/SiO$_2$) is consistent with that reported in literature.[40]

In the upper panel of Fig. 4a, the surface height and surface potential profiles of the graphene/PMMA sample are shown. By increasing the UVO treatment time from 0 to 1 to 4 min, the work function of graphene gradually increases from 4.7 to 5.1 to 5.3 eV, confirming the p-doing effect for graphene on PMMA. For the graphene/SiO$_2$/Si sample as shown in the middle panel of Fig. 4b, it is found that the work function of graphene is 4.4 eV and almost independent of the UVO treatment time. The result indicates that there is no obvious charge doping effect of the graphene on SiO$_2$/Si after the UVO treatment. For the graphene/GaN sample as shown in the lower session of Fig. 4c, the work function of graphene eventually decreases from 4.6 to 4.54 to 4.52 eV after treated by UVO from 0 to 1 to 2 min, suggesting that the doping effect is n-type.
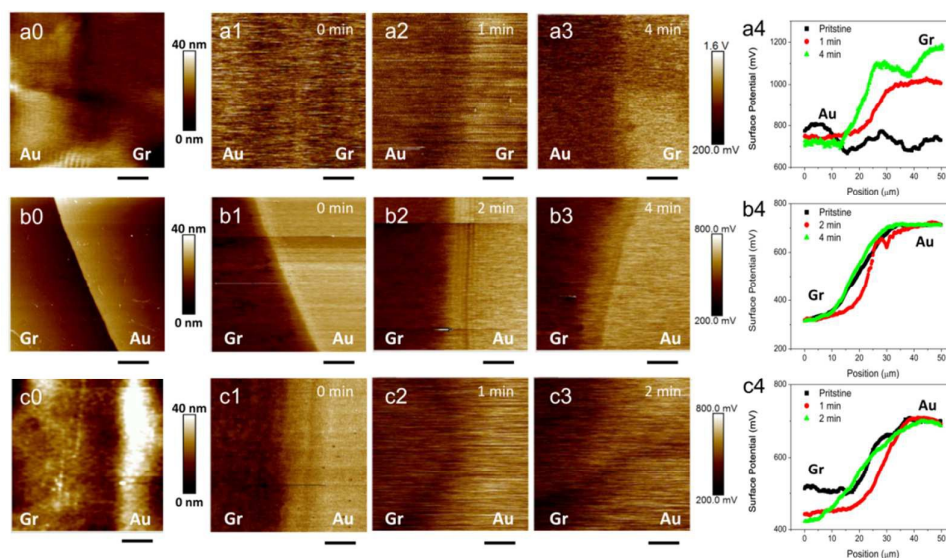
Fig. 4 Surface height and surface potential Kelvin SPM images after different time of UVO treatment. (a) Graphene on PMMA/PET substrate. (b) Graphene transferred to Si/SiO$_2$ substrate. (c) Graphene transferred to GaN substrate. The scale bar for all of the image is 1 μm.

Here, we proposed a mechanism to explain the substrate dependent doping effect as shown in Fig. 5. When the bandgap of the substrate is larger than the photon energy, e.g. PMMA, paraffin, glass and PTFE, $E_g > hv$ as shown in the upper part of the figure, there are almost no photogenerated charge carrier formation in the substrate. The graphene loses electrons to O_3 molecules and it is thus p-type doped. If the bandgap of the substrate is smaller than the photon energy, i.e. $E_g < hv$ as shown in the lower part of Fig. 5, the photogenerated carriers in the substrate can act as the electron source for the graphene, as the bottom of the conduction band lies well above the Fermi energy of the graphene. Therefore, the substrate compensates the electron loss in the graphene. If this effect is very pronounced, such as the cases for F8BT (with a high photoluminescent quantum efficiency of 80%)[41] and GaN (a direct bandgap semiconductor), the graphene will be n-doped. On the other hand, if the effect is modest, the substrate can only generate a limited amount of free electrons in the conduction band, which corresponds to the cases for Si (an indirect bandgap semiconductor) and PET (with very low photogeneration efficiency).[42] For the substrate Si/SiO₂, although there is a layer of SiO₂ between Si and graphene, the optically induced mobile charge carrier, electron or hole, can across the interface between Si and graphene, which is widely called internal photoemission (IPE) effect in the graphene-oxide-silicon stack structure.[43] The energy barrier height for electrons and holes to across SiO₂ is found to be 4.3 and 4.6 eV respectively.[44] The energy of the light used in this work with hv of 4.9 eV is larger than the barrier height, which makes the compensation effect happen. The compensation effect is not as large, and the sample will behave just like pristine graphene. There is almost no observable doping effect (see Fig. 5).
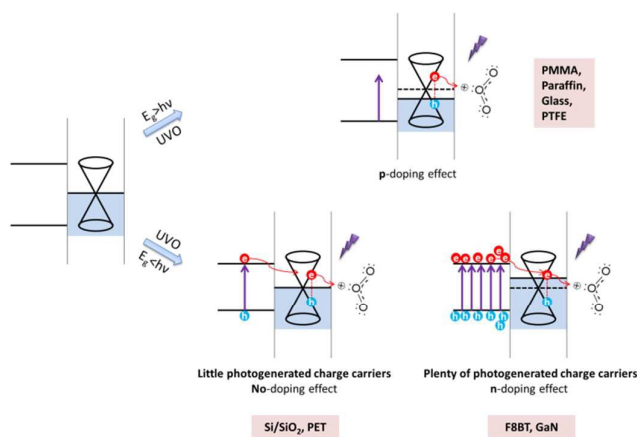
Fig. 5 Proposed substrate dependent doping mechanism of graphene by the UVO treatment.

The results in Fig. 4 are in good agreement with our proposed mechanism, where the charge doping effect is induced by the O_3 molecules with a strong electronegativity, and also dependent on the bandgap width and the quantum transition efficiency of the substrates. Nevertheless, in Fig. 3,

when the UVO exposure time is too long, which we call the second stage, the resistance of graphene increases (to different extents) for all substrates. This is because the adsorption of the ozone molecules changes from a physisorption to chemisorption, introducing epoxide groups on the graphene and significantly changing its lattice and electronic structures, drastically reducing the carrier mobility. This phenomenon is reported in previous literature as shown in Table S1. From electronic device engineering perspective, we argue that if one limits the UVO process to the first stage, an efficient charge doping effect can be easily achieved, leading to the enhanced graphene conductivity.

2.3 Stability of the charge doping effect on graphene

Raman spectroscopy is a nondestructive tool for the characterization of the number of graphene layers and the analysis of the disorder, strain and doping in graphene. We have utilized Raman spectroscopy to detect the structural damage or change in the graphene after the UVO treatment. Here, we only characterized the Raman spectra of graphene on SiO₂/Si substrate, because other substrates have strong Raman spectra peaks, it is difficult to detect the signal from graphene. Fig. 6a shows the evolution of the SiO₂/Si Raman spectra as a function of UVO exposure time from 0 to 240 s. In this figure, the graphene is seen to be of reasonably good quality. The small peak around 1345 cm⁻¹ is denoted by D, or the defect peak for graphene, whose intensity indicates the number of defects in graphene. The intensity of the D peak does not change significantly with the exposure time, indicating the UVO doping procedure is rather nondestructive or the destructive is too small to be detected by Raman. Meanwhile, the characteristic G and 2D peaks appear at around 1585 and 2680 cm⁻¹ and there are no blueshift or redshift, meaning there is almost no doping effect of the graphene on Si/SiO₂ under UVO exposure after 240 s UVO treatment. It is consistent with the previous discussion.

We have further investigated the doping stability by the UVO treatment, and the results are shown in Fig. 6b. The resistances of the five graphene/PMMA samples decrease to 30% of their pristine values after the UVO exposure for 90 s. The resistances are stable after 1 hour storage in ambient atmosphere. After 1 day, the resistances recover to the original values (before the UVO exposure). After 4 days' storage, the resistances still keep their pristine values (not shown), indicating the first stage of the UVO treatment is nondestructive or very slightly destructive. The repristination phenomenon of the resistance of graphene after UVO exposure is due to the unstable ozone adsorption on the graphene surface which is gentle and reversible. Although the doping effect from the UVO exposure does not have a long-term stability, it is stable enough for the use in nanoelectronic and optoelectronic device fabrication procedure e.g. organic light-emitting diodes. After the processing, the devices can be properly passivated so that the doping effect is secured for a long time. Furthermore, the reversible property change of the graphene enables the application of graphene in UV light detectors.
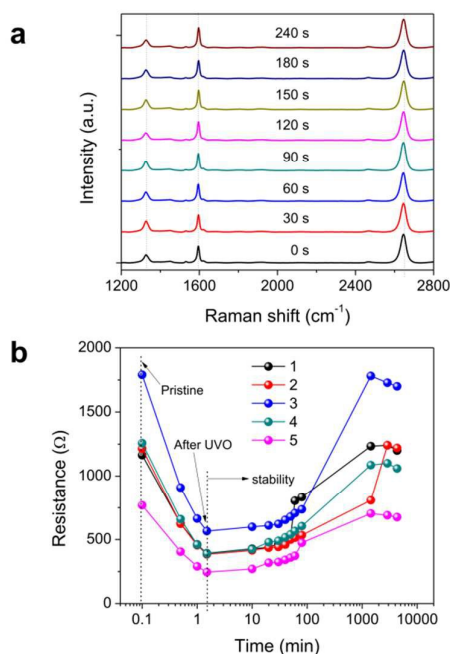
Fig. 6 (a) Raman spectra of graphene on Si/SiO$_2$ substrate exposed to UVO for different time. (b) Stability of graphene's resistivity after the UVO treatment in room atmosphere on 5 graphene/PMMA samples.

3. Conclusions

It is found that the charge doping effect on graphene by the UVO treatment is substrate dependent, where the energy bandgaps and the quantum transition efficiencies of the substrates play a key role. The resistance of graphene can be decreased by as much as 80% on F8BT, GaN and PTFE substrates, 70% on PMMA substrate, and 50% on paraffin and glass substrates. In general, wide bandgap substrates (E_g>hv) induce a p-doping effect in graphene, whereas narrow bandgap substrates (E_g<hv) with plenty of photogenerated charge carriers induce an n-doping effect. The Raman spectroscopy and doping stability tests indicate that the graphene after UVO treatment is slightly destructive and can be reversible. The as-developed UVO treatment is a convenient and highly effective method for decreasing resistance and tuning work function of graphene, which will have a great value of practical applications in the fields such as optoelectronic device transparent electrodes and photodetectors.

4. Experimental

CVD growth of graphene. The graphene was grown on 50-µm thick Cu foils in a cold-wall low-pressure CVD reactor (Black Magic, Aixtron).[45] The metal foils were heated to 1000 ^{o}C and annealed for 5 min in 50 sccm H$_2$ and 1000 sccm Ar. The actual growth was initiated by introducing CH$_4$, and maintained for 5 min. After the growth, the system was evacuated to <0.1 mbar

and cooled down. The process details were reported in our previous publications.

Post growth graphene transfer. For the graphene transfer to Si/SiO$_2$, glass, GaN and PET substrates, PMMA is used as an intermediate membrane. PMMA (950 A4, in anisole) was spin-coated on the graphene/Cu surface, and then cured at 160 ^{o}C for 5 min. A semi-rigid plastic frame was employed to provide mechanical support and facilitate the subsequent handling in the cleaning and transfer of graphene.[46] The bubbling delamination was performed in an electrolytic cell with 0.2 M NaOH solution as the electrolyte as reported.[47] Fig. 1a, c, d and g show the photograph of graphene on Si/SiO$_2$, GaN, PET, and glass substrates, respectively. For the PTFE and paraffin film substrates, the graphene/Cu stack was pressed into the substrates under 120 ^{o}C and 0.1 mbar for 5 min using Nanoimprint CNI. Then, the substrate/graphene stack was delaminated from Cu by the electrochemical bubbling method mentioned above. For multilayer graphene transfer, one only needs to repeat the processes, as shown in Fig. S1. Fig. 1f and h show the photograph of the graphene on Paraffin film and PTFE. In order to prepare the graphene on PMMA, a PMMA solution was spin-coated on the graphene/Cu, and then the PMMA (400 nm)/graphene/Cu stack was pressed into a PET substrate using Nanoimprint CNI. The PET/PMMA/graphene sample was delaminated from Cu via electrochemical bubbling method. Fig. 1e shows the photograph of the graphene on PMMA/PET substrate. For the polymer substrate F8BT, F8BT solution was spin-coated on the graphene/Cu firstly and then the F8BT/graphene was delaminated via the bubbling method. At last, the F8BT/graphene was transferred on a piece of glass. Fig. 1b shows the photograph of the graphene on F8BT/glass substrate.

Characterization. Gold electrodes with a distance of 2 mm and width of 1 mm were evaporated on the graphene as Fig. S3 shown. The resistance of graphene was measured in a two-terminal configuration. The Keithley 4200-SCS is used for electrical characterization of samples. The graphene films on SiO$_2$/Si substrates were characterized by Raman spectroscopy (Horiba XploRA) equipped with a 633 nm laser. The UVO treatment was conducted in Ozone Cleaning System (FHR UVOH 150). Oxygen gasses were channelled into the chamber at a flow rate of 0.5 slm, and two types of UV light with the wavelengths of 184.9 nm and 253.7 nm were simultaneously produced from a low pressure mercury lamp so that reactive oxygen atoms were eventually produced. The UV light power intensity is 50 mW/cm^2. The system purges O$_2$ for 1 min before the UV-lamp is turned on and the O$_2$ will continue to flow for another 3 min to purge the chamber. The surface potential of graphene was measured by SPM (Bruker Dimension Icon) in ambient environment. Doped silicon PFQNE-AL probes (Bruker) with a tip radius of 5 nm and a spring constant of 0.8 N/m were employed.

Acknowledgements

References

1 K. S. Novoselov, A. K. Geim, S. V. Morozov, D. Jiang, Y. Zhang, S. V. Dubonos, I. V. Grigorieva, A. A. Firsov, *Science* **2004**, 306, 666.
2 Y. Zhang, L. Zhang, C. Zhou, *Acc. Chem. Res,* **2013**, 46, 2329.
3 K. S. Kim, Y. Zhao, H. Jang, S. Y. Lee, J. M. Kim, K. S. Kim, J. H. Ahn, P. Kim, J. Y. Choi, B. H. Hong, *Nature* **2009**, 457, 706.
4 X. Li, Y. Zhu, W. Cai, M. Borysiak, B. Han, D. Chen, R. D. Piner, L. Colombo, R. S. Ruoff, *Nano Lett.* **2009**, 9, 4359.
5 S. Bae, H. Kim, Y. Lee, X. Xu, J. S. Park, Y. Zheng, J. Balakrishnan, T. Lei, H. R. Kim, Y. I. Song, Y. J. Kim, K. S. Kim, B. Ozyilmaz, J. H. Ahn, B. H. Hong, S. Iijima, *Nat. Nanotechnol.* **2010**, 5, 574.
6 F. Bonaccorso, Z. Sun, T. Hasan, A. C. Ferrari, *Nat. Photon.* **2010**, 4, 611.
7 S. P. Pang, Y. Hernandez, X. L. Feng, K. Mullen, *Adv. Mater.* **2011**, 23, 2779.
8 X. Huang, Z. Zeng, Z. Fan, J. Liu, H. Zhang, *Adv. Mater.* **2012**, 24, 5979.
9 J. S. Oh, K. N. Kim, G. Y. Yeom, *J. Nanosci. Nanotechnol.* **2014**, 14, 1120.
10 R. Garg, N. Dutta, N. Choudhury, *Nanomaterials* **2014**, 4, 267.
11 Kasry, M. A. Kuroda, G. J. Martyna, G. S. Tulevski, A. A. Bol, *ACS Nano* **2010**, 4, 3839.
12 K. C. Kwon, K. S. Choi, S. Y. Kim, *Adv. Funct. Mater.* **2012**, 22, 4724.
13 Y. Shi, K. K. Kim, A. Reina, M. Hofmann, L.-J. Li, J. Kong, *ACS Nano* **2010**, 4, 2689.
14 Y. Song, W. Fang, A. L. Hsu, J. Kong, *Nanotechnology* **2014**, 25, 395701.
15 X. Dong, D. Fu, W. Fang, Y. Shi, P. Chen, L. J. Li, *Small* **2009**, 5, 1422.
16 Tongay, K. Berke, M. Lemaitre, Z. Nasrollahi, D. B. Tanner, A. F. Hebard, B. R. Appleton, *Nanotechnology* **2011**, 22, 425701.
17 S. K. Lee, J. W. Yang, H. H. Kim, S. B. Jo, B. Kang, H. Bong, HyoChanLee, G. Lee, K. S. Kim, K. Cho, *ACS Nano* **2014**, 8, 7968.
18 J. Park, W. H. Lee, S. Huh, S. H. Sim, S. B. Kim, K. Cho, B. H. Hong, K. S. Kim, *J. Phys. Chem. Lett.* **2011**, 2, 841.
19 R. A. Nistor, D. M. Newns, G. J. Martyna, *ACS Nano* **2011**, 5, 3096.
20 G. Lee, B. Lee, J. Kim, K. Cho, *J. Phys. Chem. C* **2009**, 113, 14225.
21 A. Nourbakhsh, M. Cantoro, A. V. Klekachev, G. Pourtois, T. Vosch, J. Hofkens, M. H. van der Veen, M. M. Heyns, S. De Gendt, B. F. Sels, *J. Phys. Chem. C* **2011**, 115, 16619.
22 M. Z. Iqbal, A. K. Singh, M. W. Iqbal, S. Seo, J. Eom, *J. Appl. Phys.* **2012**, 111, 084307.
23 R. Larciprete, P. Lacovig, S. Gardonio, A. Baraldi, S. Lizzit, *J. Phys. Chem. C* **2012**, 116, 9900.
24 D. C. Kim, D. Y. Jeon, H. J. Chung, Y. Woo, J. K. Shin, S. Seo, *Nanotechnology* **2009**, 20, 375703.
25 Z. W. Xu, L. Chen, J. L. Li, R. Wang, X. M. Qian, X. Y. Song, L. S. Liu, G. W. Chen, *Appl. Phys. Lett.* **2011**, 98, 183112.
26 I. Childres, L. A. Jauregui, J. F. Tian, Y. P. Chen, *New J. Phys.* **2011**, 13, 205008.
27 H. Ye, Z. Gu, D. H. Gracias, *Langmuir* **2006**, 22, 1863.
28 N. Leconte, J. Moser, P. Ordejon, H. H. Tao, A. Lherbier, A. Bachtold, F. Alsina, C. M. S. Torres, J. C. Charlier, S. Roche, *ACS Nano* **2010**, 4, 4033.
29 F. GÜNeŞ, G. H. Han, H.-J. Shin, S. Y. Lee, M. Jin, D. L. Duong, S. J. Chae, E. S. Kim, F. E. I. Yao, A. Benayad, J.-Y. Choi, Y. H. Lee, *Nano* **2011**, 06, 409.
30 S. Zhao, S. P. Surwade, Z. Li, H. Liu, *Nanotechnology* **2012**, 23, 355703.
31 Y. Mulyana, M. Horita, Y. Ishikawa, Y. Uraoka, S. Koh, *Appl. Phys. Lett.* **2013**, 103, 063107.
32 K. C. Kwon, W. J. Dong, G. H. Jung, J. Ham, J.-L. Lee, S. Y. Kim, *Sol. Energy Mat. Sol. C.* **2013**, 109, 148.
33 M. Z. Iqbal, S. Siddique, M. W. Iqbal, J. Eom, *J. Mater. Chem. C* **2013**, 1, 3078.
34 Z. Luo, N. J. Pinto, Y. Davila, A. T. Charlie Johnson, *Appl. Phys. Lett.* **2012**, 100, 253108.
35 Y.-J. Lin, J.-J. Zeng, *Appl. Phys. Lett.* **2013**, 102, 183120.
36 F. Lin, S.-W. Chen, J. Meng, G. Tse, X.-W. Fu, F.-J. Xu, B. Shen, Z.-M. Liao, D.-P. Yu, *Appl. Phys. Lett.* **2014**, 105, 073103.
37 M. Hofmann, Y. P. Hsieh, K. W. Chang, H. G. Tsai, T. T. Chen, *Sci. Rep.* **2015**, 5, 17393.
38 H. Y. Park, W. S. Jung, D. H. Kang, J. Jeon, G. Yoo, Y. Park, J. Lee, Y. H. Jang, J. Lee, S. Park, H. Y. Yu, B. Shin, S. Lee, J. H. Park, *Adv. Mater.* **2016**, 28, 864.
39 S. Goniszewski, M. Adabi, O. Shaforost, S. M. Hanham, L. Hao, N. Klein, *Sci. Rep.* **2016**, 6, 22858.
40 V. Panchal, R. Pearce, R. Yakimova, A. Tzalenchuk, O. Kazakova, *Sci. Rep.* **2013**, *3*, 2597.
41 A. C. Morteani, P. Sreearunothai, L. M. Herz, R. H. Friend, C. Silva, *Phys. Rev. Lett.* **2004**, 92.
42 D. M. Taylor, T. J. Lewis, *J. Phys. D: Appl. Phys.* **1971**, 4, 1346.
43 R. Yan, Q. Zhang, O. A. Kirillov, W. Li, J. Basham, A. Boosalis, X. Liang, D. Jena, C. A. Richter, A. C. Seabaugh, D. J. Gundlach, H. G. Xing, N. V. Nguyen, *Appl. Phys. Lett.* **2013**, 102, 123106.
44 R. Yan, Q. Zhang, W. Li, I. Calizo, T. Shen, C. A. Richter, A. R. Hight-Walker, X. Liang, A. Seabaugh, D. Jena, H. Grace Xing, D. J. Gundlach, N. V. Nguyen, *Appl. Phys. Lett.* **2012**, 101, 022105.
45 J. Sun, M. T. Cole, N. Lindvall, K. B. K. Teo, A. Yurgens, *Appl. Phys. Lett.* **2012**, 100.
46 C. J. L. de la Rosa, J. Sun, N. Lindvall, M. T. Cole, Y. Nam, M. Löffler, E. Olsson, K. B. K. Teo, A. Yurgens, *Appl. Phys. Lett.* **2013**, 102, 022101.
47 Z. Y. Zhan, J. Sun, L. H. Liu, E. G. Wang, Y. Cao, N. Lindvall, G. Skoblin, A. Yurgens, *J. Mater. Chem. C* **2015**, 3, 8634.

Table of Contents Graphic
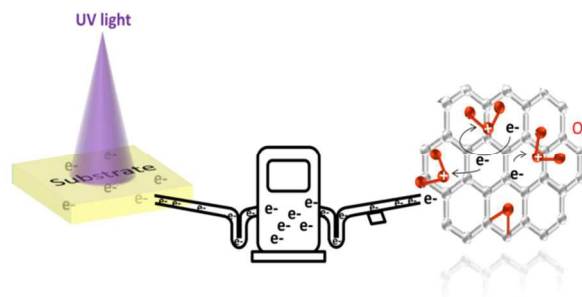
Graphene's resistance can decrease as much as 80% via UVO treatment depending on substrates' band gap and photogenerated charge carriers.